UNIVERSITÀ POLITECNICA DELLE MARCHE
Repository ISTITUZIONALE

Effect of different oleogelators on lipolysis and curcuminoid bioaccessibility upon in vitro digestion of sunflower oil oleogels

This is a pre print version of the following article:

Original
Effect of different oleogelators on lipolysis and curcuminoid bioaccessibility upon in vitro digestion of sunflower oil oleogels / Calligaris, S., Alongi, M., Lucci, P., Anese, M.. - In: FOOD CHEMISTRY. - ISSN 0308-8146. - 314:(2020). [10.1016/j.foodchem.2019.126146]

Availability:
This version is available at: 11566/308483 since: 2024-12-06T13:52:16Z

Publisher:

Published
DOI:10.1016/j.foodchem.2019.126146

Terms of use:

The terms and conditions for the reuse of this version of the manuscript are specified in the publishing policy. The use of copyrighted works requires the consent of the rights' holder (author or publisher). Works made available under a Creative Commons license or a Publisher's custom-made license can be used according to the terms and conditions contained therein. See editor's website for further information and terms and conditions.
This item was downloaded from IRIS Università Politecnica delle Marche (https://iris.univpm.it). When citing, please refer to the published version.

(Article begins on next page)

30 October 2026

Elsevier Editorial System(tm) for Food Chemistry or its open access mirror
Manuscript Draft

Manuscript Number: FOODCHEM-D-19-03433R2

Title: Effect of different oleogelators on lipolysis and curcuminoid bioaccessibility upon in vitro digestion of sunflower oil oleogels

Article Type: Research Article (max 7,500 words)

Keywords: Oleogel; Curcuminoids; Lipolysis; Bioaccessibility; Structure

Corresponding Author: Mrs. Marilisa Alongi,

Corresponding Author's Institution: University of Udine

First Author: Sonia Calligaris, Professor

Order of Authors: Sonia Calligaris, Professor; Marilisa Alongi; Paolo Lucci, Professor; Monica Anese, Professor

Abstract: Sunflower oil enriched with curcuminoid compounds (CUs) was gelled by adding 5% (w/w) saturated monoglycerides (MG), rice bran waxes (RW) or a mixture of β-sitosterol and γ-oryzanol (PS). The resulting oleogels differed for rheological properties and firmness due to the difference in gel network structure. PS oleogel was the firmest sample followed by RW and MG ones. Upon in vitro digestion, fatty acid release as a function of digestion time was greatly affected by oleogel structure: the extent of lipolysis decreased as oleogel strength increased (PS<RW<MG). On the other hand, the nature of the oleogelator affected CUs bioaccessibility, which was lower in oleogels containing crystalline particles (MG and RW). These findings appear interesting in the attempt to develop oleogels able to control lipid digestion as well as to deliver bioactive molecules in food systems.

Highlights

Sunflower oil was enriched with curcuminoids

Curcuminoid-enriched oil was gelled with different gelators

Obtained oleogels differed for rheological properties and firmness

Lypolysis kinetic during *in vitro* digestion was affected by gel structure

The type of gelator, instead of gel strength, affected curcuminoid bioaccessibility

*Manuscript
Click here to download Manuscript: Manuscript_R.docx

Effect of different oleogelators on lipolysis and curcuminoid bioaccessibility upon *in vitro* digestion of sunflower oil oleogels

Sonia Calligaris, Marilisa Alongi*, Paolo Lucci, Monica Anese

Department of Agricultural, Food, Environmental and Animal Sciences, University of Udine, Italy

*e-mail: alongi.marilisa@spes.uniud.it Tel: +39 0432-558137

Abstract

Sunflower oil enriched with curcuminoid compounds (CUs) was gelled by adding 5% (w/w) saturated monoglycerides (MG), rice bran waxes (RW) or a mixture of *β*-sitosterol and *γ*-oryzanol (PS). The resulting oleogels differed for rheological properties and firmness due to the difference in gel network structure. PS oleogel was the firmest sample followed by RW and MG ones. Upon *in vitro* digestion, fatty acid release as a function of digestion time was greatly affected by oleogel structure: the extent of lipolysis decreased as oleogel strength increased (PS<RW<MG). On the other hand, the nature of the oleogelator affected CUs bioaccessibility, which was lower in oleogels containing crystalline particles (MG and RW). These findings appear interesting in the attempt to develop oleogels able to control lipid digestion as well as to deliver bioactive molecules in food systems.

Keywords

Oleogel; Curcuminoids; Lipolysis; Bioaccessibility; Structure

1. Introduction

Oil gelation is a relatively novel strategy in which liquid oils are converted into semi-solid materials (Co & Marangoni, 2012; Patel & Dewettinck, 2016). Different oil gelators have been proposed in the literature, including low-molecular weight compounds (e.g. monoglycerides, waxes, sorbitan tristearate, 12-hydroxystearic acid, phytosterols, fatty alcohols, and fatty acids) and high-molecular weight polymers, such as ethylcellulose and chitin (Co & Marangoni, 2012; Nikiforidis & Scholten, 2015; Patel & Dewettinck, 2016; Rogers, Wright, & Marangoni, 2009; Singh, Auzanneau, & Rogers, 2017). These compounds directly gel into liquid oil by forming a self-assembly network according to different mechanisms. Most low-molecular weight gelators (e.g. monoglycerides, waxes, fatty acids, and fatty alcohols) are able to organize themselves into crystalline networks that entrap and retain oil (Co & Marangoni, 2012). The final oleogel structure strictly depends on crystal shape, number, and size, as well as on physical molecular interactions among building blocks. Differently, mixtures of phytosterols-sterol esters promote oil gelation through the formation of a supramolecular network of hollow double-walled tubules (Bot & Agterof, 2006; Calligaris, Mirolo, Da Pieve, Arrighetti, & Nicoli, 2014; Sawalha *et al*., 2015). Finally, ethylcellulose is able to form a network in oil *via* hydrogen bonding between polymer strands (Davidovich-Pinhas, 2016), whereas chitin develops a particle filled network by polymer aggregation (Nikiforidis & Scholten, 2015).

The interest in oleogels has increased dramatically in the last decade due to their potential application as replacers of common hard stock fat (i.e. saturated and trans fatty acids) in different food products (Patel & Dewettinck, 2016; Singh *et al*., 2017; Wang, Gravelle, Blake, & Marangoni, 2016). More recently, oleogels have also been proposed as efficient tools to modulate lipid digestion and deliver nutrients and bioactive molecules (O'Sullivan, Davidovich-Pinhas, Wright, Barbut, & Marangoni, 2017; Ashkar, Laufer, Rosen-Kligvasser, Lesmes, & Davidovich-Pinhas, 2019; Tan, Peh, Marangoni, & Henry, 2017a; Tan, Peh, Siow, Marangoni, & Henry, 2017b; Tan, Peh, Lau, Marangoni, & Henry, 2017c). On this topic, O'Sullivan *et al.* (2017), studying the

digestion of an ethylcellulose-based oleogel enriched with *β*-carotene, noted that oil structuring reduced lipolysis, probably by hindering lipase activity. Consequently, the residence time of *β*-carotene in the digestive tract increased leading to an evenly arrayed absorption over time with no spikes and drops in plasma concentration (O'Sullivan *et al.*, 2017). According to Yu, Shi, Liu, and Huang (2012), monostearin might increase the stability of curcuminoids loaded into oleogels, by preventing their recrystallization or precipitation (Yu *et al.*, 2012). However, these authors did not observe differences between the oleogel and the liquid oil in terms of curcuminoid bioaccessibility. The latter is expressed as the fraction of molecules enclosed in the micelles that can be potentially absorbed through the intestinal epithelium, thus becoming available for physiological functions (Ferruzzi, 2010).

Besides these studies, recently Ashkar *et al.* (2019) confirmed that oleogelation of canola oil with ethylcellulose, a *β*-sitosterol+*γ*-oryzanol mixture, or mono- and di-glycerides reduced the extent of oil lipolysis during *in vitro* digestion. As reported by these authors, such effect can be modulated by selecting the gelator type and concentration. Interestingly, also some *in vivo* studies highlighted the significant impact of lipid physical state on post-prandial plasma triglycerides, glycemia, and appetite when comparing the co-ingestion of a carbohydrate-rich meal with EC-oleogel instead of liquid oil (Tan *et al.*, 2017a, 2017b, 2017c).

Based on this evidence and with the final aim of designing food with tailor-made functionalities, it appears fundamental to improve the knowledge on the fate of oleogels and loaded bioactive molecules upon digestion. Therefore, the aim of the present study was to investigate the effect of gelator type and derived oleogel structure on oil lipolysis and on the bioaccessibility of curcuminoids (CUs) during *in vitro* digestion. Curcuminoids were chosen as model lipophilic bioactive molecules due to their weel-known health-promoting capacity (Aggarwal, Kumar, & Bharti, 2003; Aziz *et al.*, 2013; Su, Wang, & Chi, 2017; Zheng *et al.*, 2014). CUs are extracted from turmeric and include three major compounds: bisdemethoxycurcumin, demethoxycurcumin and curcumin (Shishu & Maheshwari, 2010). Although the latter is the most abundant, representing

nearly 80% of total CUs, the health-promoting capacity of the mixture of the three CUs in turmeric extract is higher than that generated by the sole curcumin (Chakravarty, Chatterjee, Yasmin, & Mazumder, 2009; Račková *et al.*, 2009). In this study, sunflower-oil and oleogels containing 5% (w/w) of gelator (saturated monoglycerides, rice-bran waxes, and *β*-sitosterol+*γ*-oryzanol mixture) were enriched with CUs and characterized for mechanical and rheological properties as well as for the CUs stability during storage. Afterward, CUs-enriched oil and oleogels were *in vitro* digested to assess lipolysis and CUs bioaccessibility.

2. Materials and methods

2.1. Materials

High oleic sunflower oil (fatty acid profile reported in Table S1) was kindly provided by Olitalia srl (Forlì, Italy) and turmeric extract (NNCL2065, ext. dry conc. std 20:1) was purchased from Network Nutrition – IMCD spa (Milan, Italy). Bisdemethoxycurcumin (BDMC), demethoxycurcumin (DMC) and curcumin (C) analytical standards, α-amylase from Bacillus sp., porcine pepsin, porcine lipase, porcine bile extract, amyloglucosidase from Aspergillus niger, HCl, NaOH, $CaCl_2(H_2O)_2$, Na_2CO_3, $NaHCO_3$, NaCl, KCl, KH_2PO_4, $MgCl_2(H_2O)_6$, $(NH_4)_2CO_3$, and $MgSO_4$ were purchased from Sigma Aldrich (Milan, Italy). Myverol™ saturated monoglycerides (fatty acid composition: 1.4% C14:0, 59.8% C16:0, 38.8% C18:0; melting point 68.05 ± 0.5 °C) were purchased from Kerry Bioscience (Bristol, UK); β-sitosterol (75.5% β-sitosterol, 12.0% β-sitostanol, 8.4% campesterol, 3.0% other) and γ-oryzanol (99% purity) were purchased from Nutraceutica srl (Monterenzio, Italy); rice wax was purchased from Kahl GmbH & Co. KG (Reinbek, Germany). All solvents were purchased from Sigma–Aldrich (Milan, Italy). Acetonitrile and 2-isopropanol were of HPLC grade. Deionized water (System advantage A10®, Millipore S.A.S, Molsheim, France) was used for all the analyses.

2.2. Methods

2.1.1. Oil enrichment

The turmeric extract was added to sunflower oil (5 mg/g, w/w) and the mixture was stirred for 2 h at 80 °C in the dark under nitrogen atmosphere, to avoid CUs and oil oxidation. The mixture was cooled to room temperature and filtered (Chromafil PET-20/25, 0.20 µm, 25 mm Düren, Germany) to remove insoluble particles.

2.1.2. Oleogel preparation

Oleogels were prepared by mixing CUs-enriched sunflower oil with 5% (w/w) of saturated monoglycerides (MG) (Da Pieve, Calligaris, Co, Nicoli, & Marangoni, 2010), rice waxes (RW) (Doan, Van De Walle, Dewettinck, & Patel, 2015), or a mixture of *β*-sitosterol and *γ*-oryzanol (PS) (2:3 w/w) (Calligaris *et al.*, 2014). The mixtures were heated under stirring in dark conditions for 30 min at 80 °C for MG and RW, and for 45 min at 90 °C for PS, until melting was reached. MG and BW samples were quiescently cooled to 20 °C and stored at this temperature. PS oloege was cooled to 4 °C and kept at this temperature for 12 hours before being stored at 20 °C. All samples were then analysed after 2 days of storage at 20 °C.

2.1.3. Oleogel storage

Aliquots of 5 g of CUs-enriched oil and oleogels were placed into 10 mL vials and stored at 20 °C under dark for increasing time. Samples were collected after 60 and 100 days and analyzed for CUs content.

2.1.4. Firmness

Oleogel firmness was determined using a texture analyzer (TA.XT Plus, Stable Micro Systems Ltd, Godalming, UK) equipped with a 5 kg load cell. Forty grams of 25-mm-thick sample were compressed with a 35-mm-diameter compression platen at a crosshead speed of 1.5 mm/s

(Giacintucci *et al.*, 2018) and firmness was expressed as the maximum force (N) applied to the samples.

2.1.5. Rheological measurement

Rheological properties of oleogels were determined with a Haake Rheostress 6000 (Thermo Scientific, Rheostress, Haake, Germany). Aliquots of about 5 g of sample were transferred on a 40-mm parallel-plate geometry system thermostated at 20 °C and the measuring gap was set at 2 mm. Samples were equilibrated for 5 min before testing to allow relaxation. Stress sweep measurement in the range of 0.1 to 1000 Pa was carried out at 1 Hz frequency to determine the linear viscoelastic region. Frequency sweep was carried out by applying a fixed stress value chosen in the linear viscoelastic region with a frequency scan of 0.1 to 10 Hz. Data were acquired and managed by applying the software Haake Rheowin v.4.60.0001 (Thermo Fisher Scientific). The critical stress was computed as the stress leading to a 10% G′ decrease during the stress sweep. G′ and G″ were compared at 1 Hz. The tangent of the phase angle (Tanδ) was computed as the ratio between the two moduli (G″/G′) during the frequency sweep.

2.1.6. Macroscopic appearance

Gel images were acquired by using an image acquisition cabinet (Immagini and Computer, Bareggio, Italy) equipped with a digital camera (EOS 550D, Canon, Milan, Italy). The digital camera was placed on an adjustable stand positioned 40 cm in front of a black cardboard base where the sample was placed. Light was provided by four 23 W frosted photographic floodlights, in a position allowing minimum shadow and glare. Other camera settings were: shutter time 1/250 s, F-Number F/2,8 and focal length 60 mm. Images were saved in jpeg format resulting in pictures of 5184 × 3456 pixels, 72 × 72 dpi.

2.1.7. Polarized light microscopy

Polarized light microscopy was carried out by using a Leica DM 2000 optical microscope under polarized light conditions (Leica Microsystems, Heerbrugg, Switzerland). A small portion of gel was placed on a glass slide, covered with a cover slide and observed at 20 °C. Images were taken at 200× magnification using a Leica EC3 digital camera and elaborated by the Leica Suite Las EZ software (Leica Microsystems, Heerbrugg, Switzerland).

2.1.8. In vitro *digestion*

In vitro digestion was carried out according to the protocol proposed by Minekus *et al*. (2014). Briefly, the simulated salivary (SSF), gastric (SGF) and intestinal (SIF) fluids were prepared and stored at 4 °C. The fluids were preheated to 37 °C just before *in vitro* digestion. The oral phase was started by adding to 0.25 g sample (oil or oleogel), 6 μL of $CaCl_2(H_2O)_2$ (0.3 M), 194 μL of water and 800 μL of a 6.4 mg/mL α-amylase solution, prepared in SSF and providing 75 U/mL activity in the final mixture. The sample was maintained at 37 °C under stirring for 2 min. At the end of the oral phase, the pH was adjusted to 3.0 with 40 μL HCl (1 M). Subsequently, 140 μL water and 1.82 mL of a 0.31 mg/mL pepsin solution, prepared in SGF and providing 2,000 U/mL activity in the final mixture, were added to start the gastric phase. The mix was stirred at 37 °C for up to 2 h. At the end of the gastric phase, the pH was adjusted to 7.0 with 30 μL NaOH (1 M). The intestinal phase was initiated by adding 8 μL $CaCl_2(H_2O)_2$ (0.3 M), 262 μL of water, 3.2 mL of 22.15 mg/mL lipase solution, prepared in SIF and providing 100 U/mL activity in the final mixture, and 0.5 mL of 160 mM bile extract prepared in SIF. The mix was stirred at 37 °C for up to 2 h. At the end of the intestinal phase, samples were centrifuged at 30,000 *g* for 70 min at 4 °C (Beckman Avanti tm J-25, Beckman Instruments Inc., Palo Alto, CA, USA) and the supernatant, i.e. the mixed micellar phase, was collected.

2.1.9. *Particle size and zeta potential of digested samples*

The particle size distribution of the mixed micellar phase of digested oil and oleogels was measured by dynamic laser light scattering (Zetasizer NanoZS, Malvern Instruments, Worcestershire, UK). Samples were diluted 1:100 (v/v) with deionized water and placed in a cell where the laser light, set at 173 ° angle, was scattered by the particles. Particle size was reported as volume-weighed mean diameter in nm. The ζ-potential was also measured by placing the diluted sample in a capillary cell equipped with two electrodes to assess particle electrophoretic mobility.

2.1.10. *Free fatty acid release*

The amount of free fatty acids (FFA) released from the sample during the intestinal phase of *in vitro* digestion was measured by using a titration method (Ahmed, Li, McClements, & Xiao, 2012). Immediately after the addition of lipase, the pH of the digestion mixture was monitored and maintained at 7.00 by adding 0.25 M NaOH. The volume of NaOH added to the sample was recorded and used to calculate the percentage of FFA released during lipolysis (Equations 1 and 2):

$$V_t = 2 \times \left[\frac{m_{oil}}{MW_{oil}} \frac{1000}{C_{NaOH}}\right] \quad \text{Equation 1}$$

$$\text{FFA (\%)} = \frac{V_e}{V_t} \times 100 \quad \text{Equation 2}$$

where V_e was the experimental volume of NaOH used for the titration, V_t was the theoretical volume required to titrate the fatty acids released by complete hydrolysis of triglycerides in the reaction vessel, assuming 2 FFA are produced for each triacylglycerol molecule (L) (Li, Hu, Du, Xiao, & McClements, 2011), m_{oil} was the mass of oil in the reaction vessel (g), MW_{oil} was the average molecular weight of sunflower oil (g mol^{-1}) and C_{NaOH} was the concentration of the sodium hydroxide (mol L^{-1}). The maximum value of free fatty acids released during digestion was determined after the plateau was reached, i.e. after 30 min from the beginning of intestinal phase. This value was considered as an indication of the maximum lipolysis and was reported as FFA_{max}.

2.1.11. Curcuminoid quantification and bioaccessibility computation

CUs-enriched oil and oleogels were diluted in isopropanol (100 μg/mL) and transferred to glass vials for UHPLC analysis, while the mixed micellar phase recovered after *in vitro* digestion, was submitted to extraction. Briefly, 2 mL of water was added to the digested samples followed by 2 mL of isopropanol. The sample was vigorously hand- shaken for 1 min and vortexed for 15 s. A mixture of salts ($MgSO_4$/NaCl 2.0:1.5, w/w) was then added and shaking was repeated under the same conditions. The resulting mixture was centrifuged at 5000 *g* for 15 min and the supernatant was recovered for UHPLC analysis.

To validate the extraction procedure for CUs analysis in digested samples, accuracy was evaluated by means of recovery experiments, analyzing digested samples fortified with three different amounts of CUs (5, 10 and 20 μg for each CUs), whereas precision, expressed as the repeatability of the method, was determined in terms of relative standard deviation (RSD) from recovery experiments at each fortification level. In all cases, the average recovery ranged from 92 to 100% with repeatability (CV%) lower than 2%, revealing the suitability of the procedure for the quantitative extraction of CUs from digested samples.

Different chromatographic conditions were employed to obtain a baseline separation of BDMC, DMC, and C. Fig. S1 shows the chromatogram of CUs in enriched oil samples obtained by applying the optimized chromatographic conditions. The UHPLC system used was a Shimadzu Prominence LC-20A coupled with a RF-20A fluorescence detector (Shimadzu, Milan, Italy). The column was an Agilent Poroshell C18 column (150 mm x 4.6 mm x 2.7 µm) thermostated at 30 °C. The mobile phase was a mixture of 0.2% aqueous phosphoric acid water and acetonitrile (85:15, v/v) at 0.45 mL/min flow rate. The excitation wavelength (λex) and emission wavelength (λem) were set a 430 and 524 nm, respectively. Standard stock solutions of BDMC (0.25 mg/mL), DMC (0.25 mg/mL) and C (0.5 mg/mL) were prepared in acetonitrile and intermediate working CUs solutions were prepared weekly from the stock standard solution by appropriate dilution with acetonitrile and

stored in the dark at 4 °C. Calibration curves were obtained for each curcuminoid (0.1 - 500 ng on column) and presented $R^2 > 0.998$ in all cases.

CUs bioaccessibility was calculated as the percentage ratio between the concentration of compound incorporated in the micelles after *in vitro* digestion and its concentration in the undigested sample.

2.1.12. Statistical analysis

Results are averages of three measurements carried out on two replicated experiments and are reported as means ± standard deviation. Analysis of variance (ANOVA) was performed using R (version 3.2.3, The R Foundation for Statistical Computing, Vienna, Austria). Bartlett's test was used to check the homogeneity of variance and the Tukey test was used to test for differences between means ($p < 0.05$).

3. Results and discussion

3.1. Oleogel physical and chemical properties

Oleogels containing sunflower oil enriched with CUs were prepared by using 5% (w/w) of saturated monoglycerides (MG), rice waxes (RW) and a mixture of *β*-sitosterol and *γ*-oryzanol (PS). This concentration was selected being effective in gelling vegetable oils as previously reported by different authors (Da Pieve *et al.*, 2010; Calligaris *et al.*, 2014; Doan *et al.*, 2015).

Table 1 shows firmness, rheological parameters (critical stress, G′, G″ and Tan*δ*), and micro- and macroscopic images of oleogels prepared by using MG, RW, and PS as oil gelators. The original stress sweep and frequency sweep curves are reported in Fig. S2. From the macroscopic images it can be noted that all samples were self-standing materials, even if with different structures. In particular, MG and RW oleogels were opaque sytems with cream-like structure, whereas the PS oleogel appeared as a transparent solid. From a rheological point of view, the gel behavior was confirmed for all samples, being the storage modulus (G′) higher than the loss modulus (G″) and Tan$\delta < 1$ (Zetzl *et al.*, 2014). Considering G′ and G″ at 1 Hz, the MG-based sample showed the lowest values, followed by PS and RW. On the other hand, PS demonstrated the highest critical

234 stress value, which represents the beginning of the non-linear region and accounts for the structure
235 breakdown required to onset flowing (Doan *et al.*, 2015).
236 As well known, G′ and G″ are indexes of the elastic and viscous behavior of the matrix,
237 respectively; whereas the critical stress is an indicator of the stress needed to break the gel network.
238 Thus, from the rheological parameters it can be concluded that, in spite of the reduced elastic
239 behavior, PS presented the highest stress resistance. This is also consistent with firmness values that
240 followed the order PS>RW>MG (Table 1).
241 These results are in agreement with those reported by Fayaz, Calligaris & Nicoli (2019). These
242 authors compared the ability of different molecules to gel sunflower oil, and attributed the different
243 gel properties to the peculiarities of the network structure formed by each oil gelator. As well
244 reported by Sawalha *et al.* (2013, 2015), *β*-sitosterol+*γ*-oryzanol self-assemble into a network by
245 alignment of cross-linked tubules into helical ribbons strongly stabilized by hydrogen bonds. The
246 dimension of these tubules is around 10 nm, which is smaller than the wavelength of visible light
247 accounting for system transparency (Bot & Agterof, 2006; Bot, Den Adel, & Roijers, 2008; Bot *et*
248 *al.*, 2011). or this reason, tubules are not detectable by using polarised light microscopy and they
249 can be imaged by SEM solely (Sawalha *et al.*, 2013). The peculiar network arrangement of *β*-
250 sitosterol+*γ*-oryzanol conferred to the system a higher stress resistance in comparison to the
251 crystalline networks formed by MG and RW. It should be remembered that the ability of these
252 molecules to gel into oil is associated to their self-assembly into crystals (Da Pieve *et al.*, 2010,
253 Doan *et al.*, 2015). As can be observed in the polarized light microscopy images (Table 1), the
254 morphology of crystals (bright areas) was different in MG and RW-based oleogels: small needle-
255 like crystals were formed in MG containing system, whereas large dendritic crystals were observed
256 in RW oleogel, in well agreement with the literature (Da Pieve *et al.*, 2010; Doan *et al.*, 2015;
257 Fayaz *et al.*, 2019). Both MG and RW crystals further aggregated mainly by hydrogen bonds, van
258 der Waals and hydrophobic forces to finally develop into three-dimensional gel network. As

demonstrated by Fayaz *et al*. (2019), the physical molecular interactions among crystal aggregates are expected to be stronger in rice wax-containing sample than in MG-based oleogel.

3.2. Curcuminoid stability

After the characterization of oleogels, further research was carried out to investigate the impact of oleogel preparation conditions on CUs content. As already mentioned, oleogels were prepared by heating oil at temperatures higher than the melting temperatures of the gelators. Being CUs sensitive to heat, their degradation could occur during oleogel preparation. The concentration of BDMC, DMC, and C in turmeric extract, enriched oil and oleogels was thus determined by UHPLC. BDMC, DMC, and C concentration in turmeric extract accounted for 10,142 ± 10 μg/g, 53,277 ± 79 μg/g and 147,761 ± 249 μg/g, respectively. As expected, C was the most abundant compound, followed by DMC and BDMC (Yu & Huang, 2012). Based on CUs concentration in the turmeric extract and in freshly prepared oil (Table 2), it can be observed that these compounds were completely solubilized during oil enrichment. BDMC, DMC and C concentration in oleogels did not differ significantly from those found in freshly prepared oil and ranged between 39 and 41; 264 and 274; 1,049 and 1,112 $\mu g/g_{oil}$, respectively. These results suggest that the preparation methodology applied to produce oleogels did not induce CUs degradation. It can be noted that BDMC, DMC, and C accounted for nearly 2%, 14% and 84% of CUs, respectively, in oil and oleogels.

Samples were further analyzed for CUs content during storage at 20 °C. As shown in Table 2, CUs concentration did not change up to 60 days of storage, whereas a significant decrease was recorded at 100 days of storage in all samples. In any case, the measured differences did not allow highlighting a clear effect of oleogel structure on CUs stability.

3.3. Physical properties, lipolysis and bioaccessibility of in vitro digested oleogels

The aim of the second part of the research was to study the effect of oil gelator type, and thus oleogel structure, on the digestive fate of oil and CUs. The particle size distribution of the micellar

phases obtained after *in vitro* digestion of oil and oleogels was firstly investigated (Fig. 1a). A multimodal particle size distribution was observed for all samples, revealing the presence of small and large particles. The smallest particle family detected in oil, PS and RW showed an average diameter ranging from 90 to 190 nm, attributable to the presence of mixed micelles formed upon digestion (Salvia-Trujillo *et al*., 2017). By observing particle size distributions, it is evident that RW and PS produced broader distributions than that observed in oil. This result suggests the formation of micelles with unhomogeneous size probably due to the fact that gel structure interfers with the digestion process (O'Sullivan *et al*., 2017). In particular, the gel network might represent a physical barrier to the access of lipase to its substrate or could directly interfere with lipid digestive components (McClements, Decker, & Park, 2009), resulting in a less efficient micelle formation. In this regard, it is important to highlight that micellarization plays a pivotal role in determining the absorption of loaded lipophilic bioactive compounds, but no correlation has been demonstrated between size and bioaccessibility (Salvia-Trujillo *et al*., 2017).

Differently, the major particle family in MG presented an average diameter of 28 nm. Such difference could be attributed to the ability of MG to act as surfactants during *in vitro* digestion, thus promoting the formation of smaller micelles (Reis *et al*., 2008).

Beside the presence of particles smaller than 200 nm, as shown in Fig. 1a, all analyzed samples also presented a particle family with an average diameter of 4,800-5,500 nm. This family is attributable to the presence of undigested lipid dropletssurrounded by anionic species, such as free fatty acids and bile salts (Salvia-Trujillo, Qian, Martín-Belloso, & McClements, 2013; Singh, Ye, & Horne, 2009; Zou *et al.*, 2016),and resulting in complex colloidal structures with negative charge (Zhang *et al.*, 2016).

The negative charge of particles in the micellar phase was confirmed by ζ-potential measurements (Fig. 1b). As well known, this parameter provides information about the surface electrical charge of particles and depends on the adsorbed species at the oil-water interfaces (Salvia-Trujillo *et al*., 2017). All digested oleogels presented negatively charged particles, with a ζ-potential ranging from

-50 to -62 mV. Unstructured oil and MG-containing oleogel were characterized by the most negatively charged micelles upon digestion, whereas RW- and PS-containing samples presented a higher ζ-potential, confirming the ability of different structuring agents to affect not only micelle size but also their surface charge (Fig. 1). To explain these results it can be speculated that some surface active species contained in RW and PS might play a role in modifying the total surface charge of the micelles. Moreover, some authors observed a relationship between the electrical charge upon digestion and the lipolysis degree (Qian, Decker, Xiao, & McClements, 2012). Lipid digestion was thus monitored by measuring free fatty acid (FFA) release during the intestinal phase of *in vitro* digestion (Fig. 2). In can be observed that the FFA release increased during digestion for all analyzed samples and reached a *plateau* within 30 min of intestinal digestion. This behavior is in agreement with literature data (McClements & Li, 2010; O'Sullivan, Barbut, & Marangoni, 2016). However, the extent of lipid digestion was significantly affected by oil structure. The unstructured oil presented the highest value of lipid digestion (FFA_{max}= 54%) in comparison with oleogels. This value agreed with literature findings, reporting a maximum lipolysis for unstructured sunflower oil around 57% (Ye *et al.*, 2019). Among oleogels, MG and RW presented similar lipolysis extents (nearly 45%), whereas PS-based oleogel showed the lowest lipolysis upon *in vitro* digestion, being 20% lower than that of oil.

These results suggest that the presence of differently structured supramolecular networks in oil affected the free fatty acid release, probably by hindering lipase access to triacylglycerol digestion sites. Thus, different oil gelators and gelation mechanisms seem to critically affect lipolysis, in agreement with results reported byAshkar *et al.* (2019) with reference to canola oil-based oleogels containing MG and PS. It should be noted that no universal conclusion on the relation between the gel strength and lipolysis can be gathered, as both gel strength (Yang *et al.*, 2018; Sawalha *et al.*, 2015) and lipolysis extent (Ye *et al.*, 2019) may be differently affected by fat composition. Still, it can be inferred that it may be possible to modulate fat digestibility and availability by selecting a proper oleogel structure. Several authors observed an interdependence between lipolysis efficiency

and micelle characteristics (Qian *et al.*, 2012; Salvia-Trujillo *et al.*, 2017). In fact, besides resulting in the highest lipolysis extent (Fig. 2), MG-containing oleogel also presented the smallest and most negatively charged mixed micelles (Fig. 1), comparable with those observed in the unstructured oil. Since these differences could affect the bioaccessibility of loaded lipophilic bioactive compounds, to get an insight into the effect of different structuring agents on this feature, CUs concentration and bioaccessibility in the *in vitro* digested oil and oleogels were assessed (Table 3). As well known, bioaccessibility measures the percent transfer of the bioactive molecules from the lipid phase to the aqueous one, in which CUs are incorporated into mixed micelles (Ferruzzi, 2010). Only CUs enclosed in the micellas are then available to be absorbed by the intestinal epithelium cells. A significant decrease ($p < 0.05$) in the concentration of CUs was observed for both oil and oleogels in the micellar phase after *in vitro* digestion, as compared to undigested samples (Table 2). Regarding the susceptibility of different CUs upon digestion, curcumin presented the lowest BAC, being more susceptible to oxidation as compared to BDMC and DMC (Gordon Luis, Ashley, Osheroff, & Schneider, 2015), in agreement with the results reported by Yu *et al.* (2011, 2012). In addition, the gelator significantly affected CUs concentration and bioaccessibility in digested samples, in contrast with the results found for the undigested oleogels (Tables 2 and 3). The bioaccessibility of CUs included into PS oleogel was comparable to that of oil ($p > 0.05$), suggesting that the tubular network did not compromise the release of CUs into digestive fluids impairing their bioaccessibility. On the other hand, oleogels structured through crystalline networks (MG- and RW-based oleogels) presented the lowest CUs content and bioaccessibility upon *in vitro* digestion. It can be speculated an effect of the presence of crystalline particles on CUs BAC. In particular, CUs could be involved in the gelation/crystallization process, being more exposed to oxygen and/or other oxidants present in the digestive mixture. To our knowledge, in the literature there are no indications on this aspect. However, some evidences show an effect of the lipid crystalline network structure on β-carotene oxidative degradation. On this regards, some authors (Calligaris, Valoppi, Barba, Anese, & Nicoli, 2018; Martins, Cerqueira, Cunha, & Vicente, 2017)

demonstrated the critical role of biomolecule location inside the lipid crystal network. Even if more research is needed on this aspect, it can be inferred that also during digestion the presence of fat crystals could impact not only the chemical stability of bioactive molecules, but also their release into the digestive fluids and thus their bioaccessibility.

4. Conclusions

Results reported in the present study confirm that oleogelation could be a profitable strategy to modulate lipid digestion while delivering bioactive molecules. Oleogel structure seems to affect the lipolysis extent and the bioaccessibility of loaded lipophilic bioactive compounds. Regarding lipid digestion, gel strength resulted critical in affecting the rate and extent of lipolysis. On the contrary, the choice of the gelling agent had an impact on CUs bioaccessibility.

Based on this knowledge, it can be suggested that oleogel development would not only offer the food industry a plastic fat replacer but could represent a strategy to modulate lipid digestion and deliver health benefits. Matching the reduction of fat uptake and the improved bioaccessibility of bioactive molecules might provide the consumers with functional foods potentially able to tackle the risk of obesity and cardiovascular diseases, currently representing major issues for public health.

Abbreviations

BDMC = bisdemethoxycurcumin; C = curcumin; CUs = curcuminoids; DMC = demethoxycurcumin; MG = monoglycerides; PS = mixture of β-sitosterol and γ-oryzanol; RW = rice wax.

Acknowledgments

The authors are grateful to Ms. Paola Netto and Mr. Alberto Tesolin for contributing to analyses.

Conflict of interest

There are no conflicts of interest to declare.

References

386 Aggarwal, B. B., Kumar, A., & Bharti, A. C. (2003). Anticancer potential of curcumin: preclinical
387 and clinical studies. *Anticancer Research, 398,* 363–398.
388 Ahmed, K., Li, Y., McClements, D. J., & Xiao, H. (2012). Nanoemulsion- and emulsion-based
389 delivery systems for curcumin: encapsulation and release properties. *Food Chemistry, 132,*
390 799–807.
391 Ashkar, A., Laufer, S., Rosen-Kligvasser, J., Lesmes, U., & Davidovich-Pinhas, M. (2019). Impact
392 of different oil gelators and oleogelation mechanisms on digestive lipolysis of canola oil
393 oleogels. *Food Hydrocolloids, 97,* 105218.
394 Aziz, M. T. A., El Ibrashy, I. N., Mikhailidis, D. P., Rezq, A. M., Wassef, M. A. A., Fouad, H. H.,
395 … Hussein, R. E. (2013). Signaling mechanisms of a water soluble curcumin derivative in
396 experimental type 1 diabetes with cardiomyopathy. *Diabetology and Metabolic Syndrome, 5,*
397 1–12.
398 Bot, A., & Agterof, W. G. M. (2006). Structuring of edible oils by mixtures of *γ*-oryzanol with *β*-
399 sitosterol or related phytosterols. *Journal of the American Oil Chemists' Society, 83,* 513–521.
400 Bot, A., Den Adel, R., & Roijers, E. C. (2008). Fibrils of *γ*-oryzanol + *β*-sitosterol in edible oil
401 organogels. *Journal of the American Oil Chemists' Society, 85,* 1127–1134.
402 Bot, A., den Adel, R., Regkos, C., Sawalha, H., Venema, P., & Flöter, E. (2011). Structuring in β-
403 sitosterol + γ-oryzanol-based emulsion gels during various stages of a temperature cycle. *Food*
404 *Hydrocolloids, 25,* 639–646.
405 Calligaris, S., Mirolo, G., Da Pieve, S., Arrighetti, G., & Nicoli, M. C. (2014). Effect of oil type on
406 formation, structure and thermal properties of *γ*-oryzanol and *β*-sitosterol-based organogels.
407 *Food Biophysics, 9,* 69–75.
408 Calligaris, S., Valoppi, F., Barba, L., Anese, M., & Nicoli, M. C. (2018). *β*-Carotene degradation
409 kinetics as affected by fat crystal network and solid/liquid ratio. *Food Research International,*
410 *105,* 599–604.
411 Chakravarty, A. K., Chatterjee, S. N., Yasmin, H., & Mazumder, T. (2009). Comparison of efficacy

412 of turmeric and commercial curcumin in immunological functions and gene regulation. *IJP -*
413 *International Journal of Pharmacology*, *5*, 333-345.
414 Co, E. D., & Marangoni, A. G. (2012). Organogels: an alternative edible oil-structuring method.
415 *Journal of the American Oil Chemists' Society*, *89*, 749–780.
416 Commission Regulation (EC) No 1333/2008 of the European Parliament and of the Council of 16
417 December 2008 on food additives.
418 Da Pieve, S., Calligaris, S., Co, E., Nicoli, M. C., & Marangoni, A. G. (2010). Shear
419 nanostructuring of monoglyceride organogels. *Food Biophysics*, *5*, 211–217.
420 Davidovich-Pinhas, M. (2016). Oleogels: a promising tool for delivery of hydrophobic bioactive
421 molecules. *Therapeutic Delivery*, *7*, 7–9.
422 Doan, C. D., Van De Walle, D., Dewettinck, K., & Patel, A. R. (2015). Evaluating the oil-gelling
423 properties of natural waxes in rice bran oil: rheological, thermal, and microstructural study.
424 *Journal of the American Oil Chemists' Society*, *92*, 801–811.
425 Doan, C. D., Tavernier, I., Okuro, P. K., & Dewettinck, K. (2018). Internal and external factors
426 affecting the crystallization, gelation and applicability of wax-based oleogels in food industry.
427 Innovative *Food Science and Emerging Technologies*, *45*, 42–52.
428 Fayaz, G., Calligaris, S., Nicoli, M.C. (2019). Comparative study on the ability of different
429 oleogelators to structure sunflower oil. *Food Biophysics*, in press, DOI 10.1007/s11483-019-
430 09597-9.
431 Ferruzzi, M. G. (2010). The influence of beverage composition on delivery of phenolic compounds
432 from coffee and tea. *Physiology & Behavior*, *100*, 33–41.
433 Giacintucci, V., Di Mattia, C. D., Sacchetti, G., Flamminii, F., Gravelle, A. J., Baylis, B., … Pittia,
434 P. (2018). Ethylcellulose oleogels with extra virgin olive oil: the role of oil minor components
435 on microstructure and mechanical strength. *Food Hydrocolloids*, *84*, 508–514.
436 Gordon, O. N., Luis, P. B., Ashley, R. E., Osheroff, N., & Schneider, C. (2015). Oxidative
437 transformation of demethoxy- and bisdemethoxycurcumin: products, mechanism of formation,

438 and poisoning of human topoisomerase IIα. *Physiology & Behavior, 28*, 989–996.
439 Gravelle, A. J., Davidovich-Pinhas, M., Zetzl, A. K., Barbut, S., & Marangoni, A. G. (2016).
440 Influence of solvent quality on the mechanical strength of ethylcellulose oleogels.
441 *Carbohydrate Polymers, 135*, 169–179.
442 Gravelle, Andrew J., Davidovich-Pinhas, M., Barbut, S., & Marangoni, A. G. (2017). Influencing
443 the crystallization behavior of binary mixtures of stearyl alcohol and stearic acid (SOSA) using
444 ethylcellulose. *Food Research International, 91*, 1–10.
445 Li, Y., Hu, M., Du, Y., Xiao, H., & McClements, D. J. (2011). Control of lipase digestibility of
446 emulsified lipids by encapsulation within calcium alginate beads. *Food Hydrocolloids, 25*,
447 122–130.
448 Martins, A. J., Cerqueira, M. A., Cunha, R. L., & Vicente, A. A. (2017). Fortified beeswax
449 oleogels: effect of β-carotene on the gel structure and oxidative stability. *Food and Function,*
450 *8*, 4241–4250.
451 McClements, D. J., Decker, E. A., & Park, Y. (2009). Controlling lipid bioavailability through
452 physicochemical and structural approaches. *Critical Reviews in Food Science and Nutrition,*
453 *49*, 48–67.
454 McClements, D. J., & Li, Y. (2010). Structured emulsion-based delivery systems: controlling the
455 digestion and release of lipophilic food components. *Advances in Colloid and Interface*
456 *Science, 159*, 213–228.
457 Minekus, M., Alminger, M., Alvito, P., Ballance, S., Bohn, T., Bourlieu, C., … Brodkorb, A.
458 (2014). A standardised static *in vitro* digestion method suitable for food – an international
459 consensus. *Food and Function, 5*, 1113–1124.
460 Mohsenin, N. N., & Mittal, J. P. (1977). Use of rheological terms and correlation of compatible
461 measurements in food texture research. *Journal of Texture Studies, 8*, 395–408.
462 Nikiforidis, C. V., & Scholten, E. (2015). Polymer organogelation with chitin and chitin
463 nanocrystals. *RSC Advances, 5*, 37789–37799.

O'Sullivan, C. M., Barbut, S., & Marangoni, A. G. (2016). Edible oleogels for the oral delivery of lipid soluble molecules: composition and structural design considerations. *Trends in Food Science and Technology, 57*, 59–73.

O'Sullivan, C. M., Davidovich-Pinhas, M., Wright, A. J., Barbut, S., & Marangoni, A. G. (2017). Ethylcellulose oleogels for lipophilic bioactive delivery-effect of oleogelation on *in vitro* bioaccessibility and stability of beta-carotene. *Food and Function, 8*, 1438–1451.

Patel, A. R., & Dewettinck, K. (2016). Edible oil structuring: an overview and recent updates. *Food and Function, 7*, 20–29.

Peyronel, F., & Campos, R. (2012). *Methods used in the study of the physical properties of fats.* In A. G. Marangoni (Ed.), Structure-function analysis of edible fats (pp. 262–277). Urbana: AOCS Press.

Pinheiro, A. C., Coimbra, M. A., & Vicente, A. A. (2016). *In vitro* behaviour of curcumin nanoemulsions stabilized by biopolymer emulsifiers - Effect of interfacial composition. *Food Hydrocolloids, 52*, 460–467.

Qian, C., Decker, E. A., Xiao, H., & McClements, D. J. (2012). Nanoemulsion delivery systems: influence of carrier oil on beta-carotene bioaccessibility. *Food Chemistry, 135*, 1440–1447.

Račková, L., Koštálová, D., Bezáková, L., Fialova, S., Bauerova, K., Toth, J., … Obložinsky, M. (2009). Comparative study of two natural antioxidants, curcumin and *Curcuma longa* extract. *Journal of Food & Nutrition Research, 48*, 148-152.

Reis, P. M., Raab, T. W., Chuat, J. Y., Leser, M. E., Miller, R., Watzke, H. J., & Holmberg, K. (2008). Influence of surfactants on lipase fat digestion in a model gastro-intestinal system. *Food Biophysics, 3*, 370–381.

Rogers, M. A., Wright, A. J., & Marangoni, A. G. (2009). Oil organogels: the fat of the future? *Soft Matter, 5*, 1594–1596.

Salvia-Trujillo, L., Qian, C., Martín-Belloso, O., & McClements, D. J. (2013). Influence of particle size on lipid digestion and beta-carotene bioaccessibility in emulsions and nanoemulsions.

Food Chemistry, *141*, 1475–1480.

Salvia-Trujillo, L., Verkempinck, S. H. E., Sun, L., Van Loey, A. M., Grauwet, T., & Hendrickx, M. E. (2017). Lipid digestion, micelle formation and carotenoid bioaccessibility kinetics: influence of emulsion droplet size. *Food Chemistry*, *229*, 653–662.

Sawalha, H., Margry, G., den Adel, R., Venema, P., Bot, A., Flöter, E., & van der Linden, E. (2013). The influence of the type of oil phase on the self-assembly process of γ-oryzanol + β-sitosterol tubules in organogel systems. *European Journal of Lipid Science and Technology*, *115*, 295–300.

Sawalha, H., Venema, P., Bot, A., Flöter, E., Den Adel, R., & Van Der Linden, E. (2015). The phase behavior of γ-oryzanol and β-sitosterol in edible oil. *JAOCS, Journal of the American Oil Chemists' Society, 92*, 1651–1659.

Shishu, & Maheshwari, M. (2010). Comparative bioavailability of curcumin, turmeric and Biocurcumax in traditional vehicles using non-everted rat intestinal sac model. *Journal of Functional Foods*, *2*, 60–65.

Singh, A., Auzanneau, F. I., & Rogers, M. A. (2017). Advances in edible oleogel technologies – A decade in review. *Food Research International*, *97*(March), 307–317.

Singh, H., Ye, A., & Horne, D. (2009). Structuring food emulsions in the gastrointestinal tract to modify lipid digestion. *Progress in Lipid Research*, *48*, 92–100.

Su, L., Wang, Y., & Chi, H. (2017). Effect of curcumin on glucose and lipid metabolism, FFAs and TNF-α in serum of type 2 diabetes mellitus rat models. *Saudi Journal of Biological Sciences*, *24*, 1776–1780.

Tan, S.-Y., Peh, E., Marangoni, A. G., & Henry, C. J. (2017a). Effects of liquid oil vs. oleogel co-ingested with a carbohydrate-rich meal on human blood triglycerides, glucose, insulin and appetite. *Food and Function*, *8*, 241–249.

Tan, S. Y., Peh, E., Siow, P. C., Marangoni, A. G., & Henry, C. J. (2017b). Effects of the physical-form and the degree-of-saturation of oil on postprandial plasma triglycerides, glycemia and

appetite of healthy Chinese adults. *Food and Function, 8*, 4433–4440.

Tan, S.-Y., Peh, E., Lau, E., Marangoni, A. G., & Henry, C. J. (2017c). Physical form of dietary fat alters postprandial substrate utilization and glycemic response in healthy chinese men. *The Journal of Nutrition, 147*, 1138–1144.

Verkempinck, S. H. E., Moens, L. G., Charleer, L., Loey, A. M. Van, & Hendrickx, M. E. (2018). Emulsion stability during gastrointestinal conditions effects lipid digestion kinetics. *Food Chemistry*, *246*, 179–191.

Wang, F. C., Gravelle, A. J., Blake, A. I., & Marangoni, A. G. (2016). Novel trans fat replacement strategies. *Current Opinion in Food Science*, *7*, 27–34.

Yang, S., Zhu, M., Wang, N., Cui, X., Xu, Q., Saleh, A. S. M., … Xiao, Z. (2018). Influence of oil type on characteristics of β-sitosterol and stearic acid based oleogel. *Food Biophysics, 13*, 362–373.

Ye, Z., Cao, C., Li, R., Cao, P., Li, Q., & Liu, Y. (2019). Lipid composition modulates the intestine digestion rate and serum lipid status of different edible oils: a combination of *in vitro* and *in vivo* studies. *Food and Function, 10*, 1490–1503.

Yu, H., Li, J., Shi, K., & Huang, Q. (2011). Structure of modified e-polylysine micelles and their application in improving cellular antioxidant activity of curcuminoids. *Food and Function, 2*, 373–380.

Yu, H., & Huang, Q. (2012). Improving the oral bioavailability of curcumin using novel organogel-based emulsions. *Journal of Agricultural and Food Chemistry*, *60*, 5373–5379.

Yu, H., Shi, K., Liu, D., & Huang, Q. (2012). Development of a food-grade organogel with high bioaccessibility and loading of curcuminoids. *Food Chemistry, 131*, 48–54.

Zetzl, A. K., Gravelle, A. J., Kurylowicz, M., Dutcher, J., Barbut, S., & Marangoni, A. G. (2014). Microstructure of ethylcellulose oleogels and its relationship to mechanical properties. *Food Structure*, *2*, 27–40.

Zhang, R., Zhang, Z., Zou, L., Xiao, H., Zhang, G., Decker, E. A., & McClements, D. J. (2016).

Impact of lipid content on the ability of excipient emulsions to increase carotenoid bioaccessibility from natural sources (raw and cooked carrots). *Food Biophysics*, *11*, 71–80.

Zheng, A., Li, H., Feng, Z., Wu, J., Cao, K., Wang, X., … Zhou, B. (2014). Anticancer effect of a curcumin derivative B63: ROS production and mitochondrial dysfunction. *Current Cancer Drug Targets*, *14*, 156–166.

Zou, L., Zheng, B., Zhang, R., Zhang, Z., Liu, W., Liu, C., … McClements, D. J. (2016). Influence of lipid phase composition of excipient emulsions on curcumin solubility, stability, and bioaccessibility. *Food Biophysics*, *11*, 213–225.

Captions for figures

Fig. 1. Particle size distribution (a) and ζ-potential (b) of oil and oleogels obtained by using 5% (w/w) of monoglycerides (MG), rice wax (RW) and phytosterols (PS), after *in vitro* digestion. Different letters (a-c) mean significant differences ($p < 0.05$) among samples.

Fig. 2. Concentration of free fatty acids (FFA) during *in vitro* digestion of oil and oleogels containing 5% (w/w) of monoglycerides (MG), rice wax (RW) or phytosterols (PS). Different letters (a-c) mean significant differences ($p < 0.05$) among samples.

Fig. S1. UHPLC trace of CUs enriched oil. 1: bisdemethoxycurcumin; 2: demethoxycurcumin; 3: curcumin.

Fig. S2. Stress and frequency sweep curves of monoglyceride- (MG), rice wax- (RW) and phytosterol- (PS) based oleogels.

*Declaration of Interest Statement

DECLARATION OF INTEREST

We wish to confirm that there are no known conflicts of interest associated with this publication and there has been no significant financial support for this work that could have influenced its outcome.

We confirm that the manuscript has been read and approved by all named authors and that there are no other persons who satisfied the criteria for authorship but are not listed. We further confirm that the order of authors listed in the manuscript has been approved by all of us.

We confirm that we have given due consideration to the protection of intellectual property associated with this work and that there are no impediments to publication, including the timing of publication, with respect to intellectual property. In so doing we confirm that we have followed the regulations of our institutions concerning intellectual property.

We understand that the Corresponding Author is the sole contact for the Editorial process (including Editorial Manager and direct communications with the office). She is responsible for communicating with the other authors about progress, submissions of revisions and final approval of proofs. We confirm that we have provided a current, correct email address which is accessible by the Corresponding Author.

Udine, 15th May 2019

Signed by all authors as follows:

Sonia Calligaris

Marilisa Alongi

Paolo Lucci

Monica Anese

Author contribution

Sonia Calligaris: Conceptualization, Writing - Review & Editing, Supervision; Marilisa Alongi: Investigation, Formal analysis, Writing - Original Draft; Paolo Lucci: Methodology, Validation, Writing - Review & Editing; Monica Anese: Writing - Review & Editing, Supervision.

Table 1

Table 1

Firmness, G', G'', Tanδ, critical stress, and microscopic and macroscopic images of oleogels obtained by using 5% (w/w) of monoglycerides (MG), rice wax (RW) and phytosterols (PS).

Gelling agent	Firmness (N)	G' (Pa)	G" (Pa)	Tanδ	Critical stress (Pa)	Microscopic appearance	Macroscopic appearance
MG	0.91 ± 0.08 [c]	25090 ± 4044 [b]	3075 ± 513 [b]	0.15 ± 0.01 [b]	6.6 ± 0.1 [b]	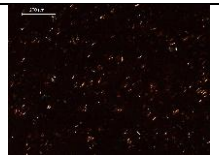	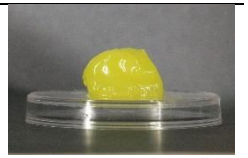
RW	3.49 ± 0.24 [b]	37413 ± 2591 [a]	4384 ± 539 [ab]	0.15 ± 0.01 [b]	16.7 ± 3.1 [b]	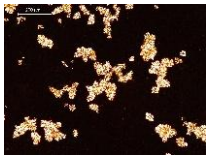	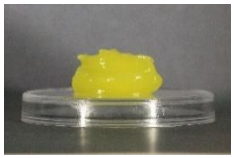
PS	5.65 ± 0.42 [a]	29410 ± 4646 [ab]	6026 ± 808 [a]	0.21 ± 0.01 [a]	128.5 ± 28.6 [a]	n.a.	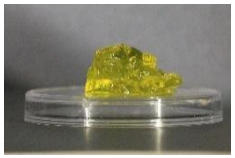

Different letters (a-c) mean significant differences ($p < 0.05$) of structural properties among oleogels.
n.a. Images not acquired.

Table 2

Table 2

Bisdemethoxycurcumin (BDMC), demethoxycurcumin (DMC) and curcumin (C) contents in oil and oleogels obtained by using 5% (w/w) of monoglycerides (MG), rice wax (RW) and phytosterols (PS), during storage at 20 °C under dark.

	BDMC ($\mu g/g_{oil}$)			DMC ($\mu g/g_{oil}$)			C ($\mu g/g_{oil}$)		
Sample	0 days	60 days	100 days	0 days	60 days	100 days	0 days	60 days	100 days
Oil	$41.2 \pm 1.8^{A,a}$	$38.5 \pm 0.2^{A,a}$	$31.6 \pm 0.1^{B,a}$	$274 \pm 12^{A,a}$	$251 \pm 1^{A,a}$	$193 \pm 3^{B,b}$	$1112 \pm 48^{A,a}$	$974 \pm 5^{B,a}$	$820 \pm 5^{C,b}$
MG	$39 \pm 1.5^{A,a}$	$38.9 \pm 1.8^{A,a}$	$32.1 \pm 0.3^{A,a}$	$268 \pm 10^{A,a}$	$250 \pm 12^{A,a}$	$192 \pm 2^{A,b}$	$1049 \pm 38^{A,a}$	$974 \pm 49^{A,a}$	$812 \pm 6^{B,bc}$
RW	$41.0 \pm 2.8^{A,a}$	$37.3 \pm 0.3^{A,a}$	$29.8 \pm 0.2^{B,b}$	$272 \pm 15^{A,a}$	$246 \pm 1^{A,a}$	$200 \pm 2^{B,ab}$	$1104 \pm 57^{A,a}$	$968 \pm 2^{A,a}$	$794 \pm 3^{B,c}$
PS	$39.7 \pm 2.3^{A,a}$	$38.2 \pm 0.3^{A,a}$	$31.3 \pm 0.2^{B,a}$	$265 \pm 15^{A,a}$	$247 \pm 2^{A,a}$	$207 \pm 1^{B,a}$	$1079 \pm 58^{A,a}$	$1007 \pm 8^{A,a}$	$853 \pm 3^{B,a}$

Different capital letters (A-C) mean significant differences of curcuminoid concentration during storage. Different lowercase letters (a-c) mean significant differences ($p < 0.05$) of curcuminoid concentration between oil and oleogels.

Table 3

Table 3

Bisdemethoxycurcumin (BDMC), demethoxycurcumin (DMC) and curcumin (C) content and bioaccessibility (BAC) in oil and oleogels obtained by using 5% (w/w) of monoglycerides (MG), rice wax (RW) and phytosterols (PS) after *in vitro* digestion.

Sample	BDMC		DMC		C	
	Concentration ($\mu g/g_{oil}$)	BAC (%)	Concentration ($\mu g/g_{oil}$)	BAC (%)	Concentration ($\mu g/g_{oil}$)	BAC (%)
Oil	22.9 ± 3.8 ^{a}	55.6 ± 9.1 ^{a}	141.9 ± 22.8 ^{a}	51.7 ± 8.3 ^{a}	520.4 ± 85.9 ^{a}	50.4 ± 7.7 ^{a}
MG	13.1 ± 0.5 ^{c}	33.6 ± 1.4 ^{b}	87.3 ± 5.5 ^{b}	32.5 ± 2.1 ^{c}	333.9 ± 31.5 ^{b}	31.8 ± 3.0 ^{b}
RW	13.7 ± 3.4 ^{bc}	33.3 ± 8.4 ^{b}	94.0 ± 22.6 ^{b}	34.5 ± 8.3 ^{bc}	376.5 ± 93.0 ^{ab}	29.2 ± 8.4 ^{b}
PS	20.5 ± 2.0 ^{ab}	51.4 ± 5.0 ^{a}	130.5 ± 11.1 ^{ab}	49.1 ± 4.2 ^{ab}	489.3 ± 39.7 ^{ab}	45.2 ± 3.7 ^{a}

Different letters (a-c) mean significant differences ($p < 0.05$) of curcuminoid concentration or bioaccessibility among samples.

Figure 1

Click here to download Figure(s): Fig. 1.docx

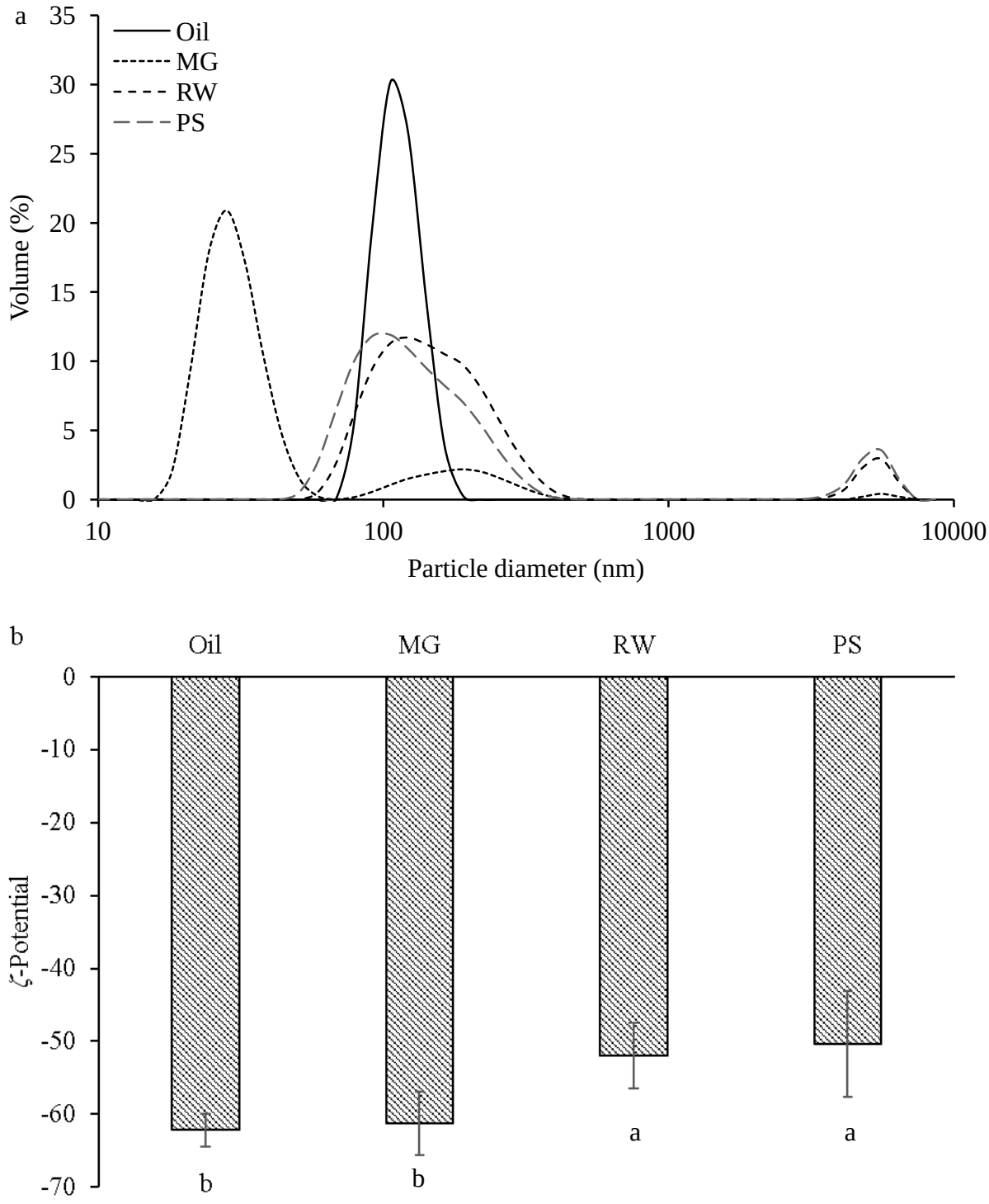

Fig. 1

Figure 2

Click here to download Figure(s): Figure 2_R.docx

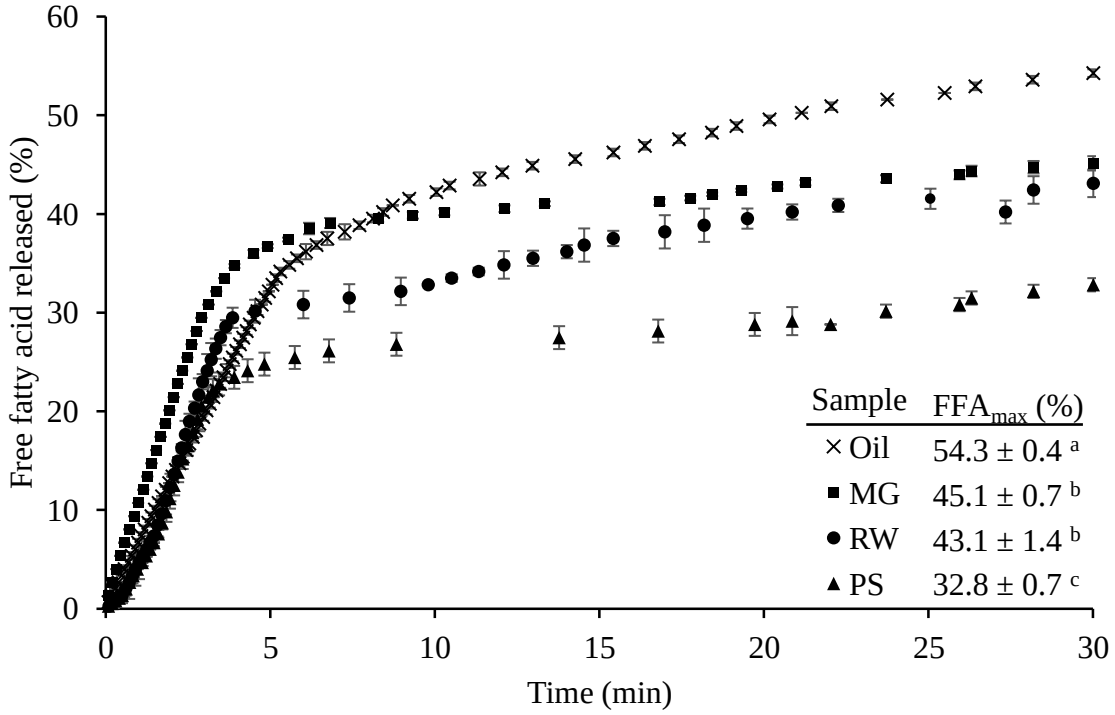

Fig. 2.

Supplementary Material_Table S1
Click here to download Supplementary Material: Table S1.docx

Table S1

Total fatty acid profile of high-oleic sunflower oil

Fatty acid	Relative abundance (%)
C16:0	5.1 ± 1.0
C16:1 $^{\Delta 9c}$	0.2 ± 0.0
C18:0	3.0 ± 0.1
C18:1$^{\Delta 9c}$	81.6 ± 1.5
C18:2 $^{\Delta 9c,12c}$	8.3 ± 0.8
C18:3 $^{\Delta 9c,12c,15c}$	0.2 ± 0.0
C20:0	0,3 ± 0.0
C20:1 $^{\Delta 11}$	0.3 ± 0.1
C22:0	1.1 ± 0.2

Legend for fatty acids – m:n Δx, m=number of carbon atoms, n= number of double bonds, x= position of double bonds.

Supplementary Material_Fig. S2

Click here to download Supplementary Material: Fig. S2.docx

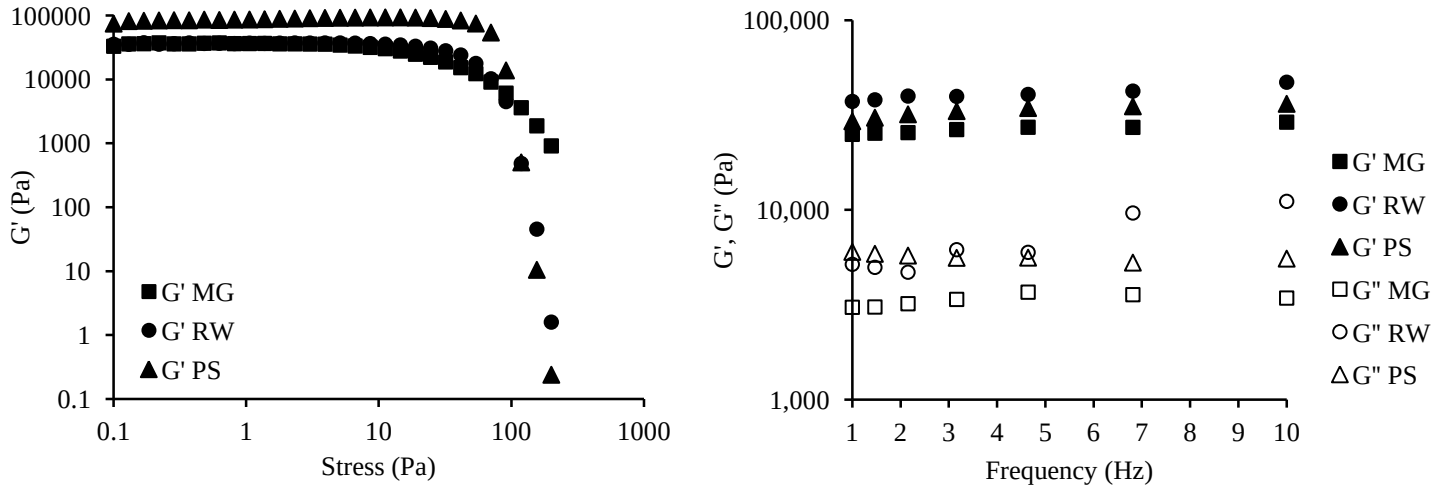

Fig. S2